

Modelling of Heat Transfer Characteristics around a Cylindrical-Barrier

Olalekan Adebayo Olayemi⁽¹⁾, Abdulganiyu Salaudeen⁽¹⁾, Khaled Al-Farhany⁽²⁾, Rasaq Olawale Medupin⁽³⁾, Isaac Kayode Adegun⁽⁴⁾

⁽¹⁾ Department of Aeronautics and Astronautics, Faculty of Engineering and Technology, Kwara State University, Malete, Kwara State, NIGERIA

⁽²⁾ Department of Mechanical Engineering, University of Al-Qadisiyah, Al-Qadisiyah, IRAQ

⁽³⁾ Department of Materials and Metallurgical Engineering, Federal University of Technology, Owerri, Imo State, NIGERIA

⁽⁴⁾ Department of Mechanical Engineering, Faculty of Engineering and Technology, University of Ilorin, Ilorin, NIGERIA

e-mails: olalekan.olayemi@kwasu.edu.ng; khaled.alfarhany@qu.edu.iq; rasaq.medupin@futo.edu.ng; kadegun@unilorin.edu.ng

SUMMARY

Numerical analysis of fluid flow and natural convection heat transfer of Fe_3O_4 -water nanofluid around a heated rectangular cylindrical barrier placed in a square cavity was conducted using COMSOL Multiphysics 5.5 software. The effects of nanoparticles volume fraction ($0 \leq \phi \leq 0.06$), aspect ratio ($0.1 \leq AR \leq 0.7$), and Rayleigh number ($10^2 \leq Ra \leq 10^6$) on heat transfer and fluid flow due to natural convection in the cavity were analyzed. The heated rectangular cylinder walls were set to have a higher constant temperature while the enclosure walls were maintained at a lower fixed temperature. Results are reported in form of velocity streamlines, isothermal contours, local and average Nusselt numbers. Also, the average Nusselt number for all the walls of the heated rectangular cylinder was found to be independent of Rayleigh number in the range of $10^2 \leq Ra \leq 10^3$ for the various nanoparticle volume fractions ($0 \leq \phi \leq 0.06$) considered. Furthermore, the average Nusselt number of the walls of the cylinder increases with increasing Rayleigh number and aspect ratio.

KEYWORDS: cylindrical barrier; fluid flow; heat transfer; modelling; nanofluid; natural convection.

1. INTRODUCTION

Cooling enhancement via convective heat transfer of materials like water, ethylene glycol, motor oil, alumina, copper, and silver has been broadly utilized in various significant fields, such as ventilating, heating, cooling framework (systems), small scale gadgets, transportation, and fabrication [1-3]. Recently, fluids combined with nano-metric-sized particles to form nanofluids have been considered by several researchers, some of which include: Kefayati [4] that studied the heat transfer characteristics of copper (Cu), cupric

oxide (CuO), and alumina (Al₂O₃) nanoparticles. It was concluded that alumina (Al₂O₃) nanoparticles exhibited the lowest heat transfer rate and copper (Cu) nanoparticles enhanced heat transfer more than the other nanoparticles considered. Nidhin [5] investigated a similar problem for Al₂O₃ and TiO₂ nanoparticles only. Different thermal boundary conditions were imposed across the walls. Acharya and Dash [6] studied the natural convection of water-based non-Newtonian power-law nanofluid in a cavity. The side walls were in a wavy form and maintained at different constant temperatures. Sivasankaran and Pan [7] researched on free convection of nanofluid in a cavity with nonuniform temperature distributions on the sidewalls and concluded that when the amplitude ratio and the phase deviation of the sinusoidal temperature distribution were varied, the heat transferred significantly affected the heated wall, while a little effect can be seen on the other walls.

Many researchers have studied the natural convection heat transfer of a nanofluid in a partially heated enclosure such as [8, 9]. However, Sheikhzadeh et al. [8] studied the effect of partially heated walls by a heat source and a heat sink along the sidewalls of a square cavity filled with Cu-water nanofluid. While, Oztop and Abu-Nada [9] investigated the heat transfer rate of a partially heated left sidewall of a horizontal rectangular enclosure by varying the height of the heat source, the distance between the middle of the heat source, and the bottom wall of the enclosure for different nanoparticles. Revnic et al. [10] considered the effect of variable viscosity on natural convection in a rectangular cavity filled with CuO-water nanofluids. The viscosity has been assumed as a variable that depends on the nanoparticle volume fraction and temperature. The results submitted that both coefficients of heat transfer and flow of fluid were affected by the volume fraction of the nanoparticle and Rayleigh number. Alloui et al. [11] examined a rectangular enclosure with a heated bottom wall for different nanoparticles (Ag, Cu, CuO, Al₂O₃, and TiO₂). Some of their conclusions were that nanoparticles in a fluid reduce the flow field strength, especially at lower Rayleigh numbers.

In a much earlier study by Abu-Nada [12], who considered horizontal annuli using Al₂O₃ - water, a higher temperature was imposed on the inner cylinder while a lower temperature was maintained on the outer cylinder. Also, many researchers studied the natural/mixed convection of nanofluids around a solid block in a square enclosure [13-15]. They analyzed the effects of varying aspect ratios on heat transfer augmentation. Ali and Kahwaji [16] researched on a similar case as [13, 14]; water was used as the base fluid while copper was used as the nanoparticle and concluded that the mean Nusselt number was gradually enhanced as the volume fraction of the nanofluid increased from 0% to 2% for different Rayleigh numbers. Unlike those experimenting with a single obstacle, Pordanjani et al. [17], using a different approach, considered a scenario where two isothermal obstacles were used in a cavity filled with Al₂O₃-water nanofluid in the presence of a magnetic field under a buoyancy-driven flow condition. Their research showed that flow velocity, as well as Nusselt number at all nanoparticle volume fractions, decreases as Hartman number increases. It was also discovered that an inverse relation exists between Nusselt number and aspect ratio. However, the Nusselt number increased with the angle of the magnetic field and the Rayleigh number enhancement.

Mahmoudi et al. [18] presented a study of free convection cooling of a heat source attached horizontally to the left wall of the enclosure, which was kept at a constant temperature, while others were set to be adiabatic. The length of the heat source was varied in order to investigate its effect in the enclosure and its location at different Rayleigh numbers and

volume fractions of the nanoparticles. Their results indicated that at a definite heat source geometry and for a given Rayleigh number, the mean Nusselt number linearly increased as the volume fraction of the nanoparticle increased. Mohebbi et al. [19, 20] used the Lattice Boltzmann method (LBM) for two different investigations at different times. Mohebbi et al. [19] examined the thermal and fluid flow behaviours in a U-shaped cavity filled with Al_2O_3 -water or TiO_2 -water nanofluid having a hot rectangular obstacle at its bottom. The cavity aspect ratio, Rayleigh number, obstacle height, and the nanoparticles volume fraction were simulated. Also, Mohebbi et al. [20] examined nanofluid natural convection in a baffled U-shaped enclosure with magnetic field presence. The effects of Hartmann number, Rayleigh number, nanoparticles volume fraction, and aspect ratio of the cavity were reported.

Gibanov et al. [21] used both the finite difference and lattice Boltzmann methods to investigate natural convection heat transfer in an enclosure with inbuilt energy sources and concluded that the lattice Boltzmann method (LBM) is more effective for solving problems of natural convection in an enclosure with or without a local heat source. Khakrah et al. [22] also employed the Lattice Boltzmann method (LBM) to analyze buoyancy-driven heat transfer in a multi-pipe sinusoidal-wall enclosure filled with Al_2O_3 -EG nanofluid. Lattice Boltzmann analysis on double-diffusive natural convection of viscoplastic fluid in a porous enclosure was studied by Kefayati [23]. Nemati et al. [24] investigated magnetic field effects on natural convection heat transfer in a closed rectangular cavity filled with nanofluid. Their results showed that convection weakens in the cavity when Darcy number decreases, but heat transfer was, however, reported to increase as porosity increases. The effects of the inclination angle on the natural convection of nanofluid in an inclined cavity and the influence of conductive curved partition and magnetic field on buoyancy flow were reported [25-29].

Natural convection of nanofluid filled in an enclosure with heated shapes using incompressible smoothed particle hydrodynamics was carried out by Raizah and Aly [30]; they concluded that as Rayleigh number increased, the streamline strength also increased, and the buoyancy flow became stronger in the cavity. While Shafee et al. [31] performed a similar investigation on a circular porous cavity with magnetic field using Fe_3O_4 -water nanofluid, Toosi and Siavashi [32] and a host of other researchers such as [33-38] studied the effects of porous layer thickness on heat transfer with a nanofluid filled porous cavity. Their analyses were predicated on the two-phase mixture of natural convection in the cavity. Bondareva et al. [39] investigated the influence of thermophoresis and Brownian diffusion in a partially opened trapezoidal cavity filled with water-based nanofluid. It was concluded that an increase in Rayleigh number leads to increased cooling of the cavity with the change in volume fraction of nanoparticles.

Ahmed et al. [40] carried out a comparative study on circular and arc cavities filled with Cu-water nanofluid using Galerkin's weighted residual finite element procedure for the investigation. The circular cavity presented a higher heat transfer rate than that of the arc cavity. Large-eddy simulations of buoyancy-driven heat transfer in a closed cavity were studied, and the results were compared with experimental data by Pilkington and Rosic [41]. Bouchoucha et al. [42] studied the influence of non-isothermal heating of a cavity with a thick bottom wall filled with nanofluid. In the investigation, Al_2O_3 -water nanofluid was used for the natural convection simulation. It was opined that nanoparticles have a positive effect on heat transfer augmentation. Boulahia et al. [43] separately investigated mixed and natural convection in a square cavity with cooling and heating circular cylinders filled with Cu-water-based nanofluid. One of their findings indicated that when Rayleigh number and size

of the circular heating cylinder increase, the heat transfer rate also increases. In another study conducted by Yu et al. [44], molten salt nanofluid was used to analyze 3-D natural convection in a heated bottom cylindrical cavity. Sannad et al. [45] reported the influence of section dimension heating on buoyancy flow in a three-dimensional enclosure having a partially heated wall filled with nanofluid. Many researchers such as [46-48] analyzed the rate of heat transfer and fluid flow characteristics using a mixture of two or more nanoparticles, while Olayemi et al. [49] gave insight into heat transfer and fluid flow around a rectangular cylinder located in a square domain using air as the working fluid.

Based on the presented extensive literature review, most of the numerical investigations conducted focused on natural convection largely in square enclosures without inner heat sources, while some have heated circular or square objects fitted to it. However, to the author's knowledge, there is no numerical study that had investigated natural convection in a square cavity filled with nanofluids with the effect of a heated rectangular block. Therefore, the current research work focuses on the effects of aspect ratio ($0.1 \leq AR \leq 0.7$), Rayleigh number ($10^2 \leq Ra \leq 10^6$), and nanofluid volume fraction ($0 \leq \phi \leq 0.06$) on the fluid flow and natural convective heat transfer characteristics of Fe_3O_4 -water nanofluid around a heated rectangular cylindrical barrier placed concentrically inside a square cavity.

2. METHODOLOGY

2.1 DESCRIPTION OF THE PHYSICAL MODEL

Figure 1(a) shows the physical model and the coordinate system adopted for the current investigation, and Figure 1(b) displays the mesh distribution of the physical model. The model comprises a rectangular cylinder (having aspect ratio, $R = \frac{w}{L}$) that is concentrically located inside a square enclosure with side length L . The cavity between the enclosure and the rectangular cylinder was filled with Fe_3O_4 -water nanofluid. The fluid flow and heat transfer are assumed to be steady and 2-dimensional. The flow characteristics in the cavity are also taken to be laminar with natural convection flow mechanism. The boundaries of the enclosure are fixed at a constant temperature of T_c . The rectangular cylinder is also assumed to be at a constant temperature of T_h . The thermodynamic fluid properties are presumed to be constant except density, which obeys the Boussinesq estimation. The solid boundaries are assumed to be stationary and the Fe_3O_4 -water mixture in equilibrium, and therefore, a single-phase model was employed for the analysis.

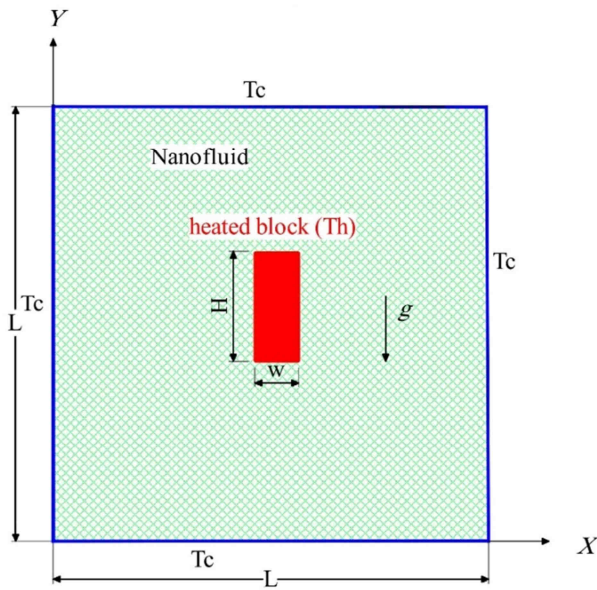


Fig. 1 (a) Physical Model

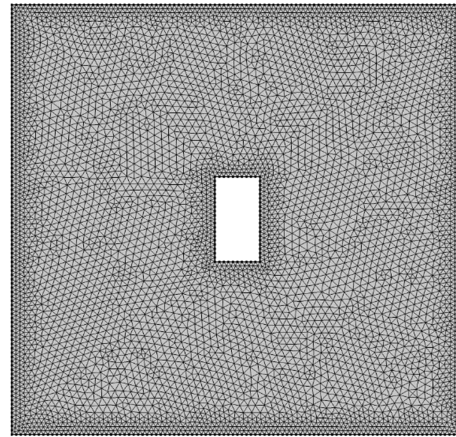


Fig. 1 (b) Mesh distribution

The thermophysical properties of the base fluid and the nanoparticle are given in Table 1.

Table 1 Thermodynamic properties of water and Fe₃O₄ nanoparticles [31]

Properties	Pure water	Fe ₃ O ₄
ρ [kgm^{-3}]	997.1	5200
C_p [$KJkg^{-1}K^{-1}$]	4179	670
k [$Wm^{-1}K^{-1}$]	0.613	6
d_p [nm]	–	47

2.2 GOVERNING EQUATIONS

The dimensional equations governing the flow physics for natural convection and the fluid flow of base fluid and nanoparticles inside a cavity using the Boussinesq estimation are given by [5]:

Continuity:

$$\frac{\partial u}{\partial x} + \frac{\partial v}{\partial y} = 0 \tag{1}$$

x-Momentum:

$$u \frac{\partial u}{\partial x} + v \frac{\partial u}{\partial y} = -\frac{\partial p}{\partial x} + \mu_{nf} \left[\frac{\partial^2 u}{\partial x^2} + \frac{\partial^2 u}{\partial y^2} \right] \tag{2}$$

y-Momentum:

$$u \frac{\partial v}{\partial x} + v \frac{\partial v}{\partial y} = -\frac{\partial p}{\partial y} + \mu_{nf} \left[\frac{\partial^2 v}{\partial x^2} + \frac{\partial^2 v}{\partial y^2} \right] + g(\rho\beta)_{nf} (T - T_c) \tag{3}$$

Energy:

$$u \frac{\partial T}{\partial x} + v \frac{\partial T}{\partial y} = \alpha_{nf} \left[\frac{\partial^2 T}{\partial x^2} + \frac{\partial^2 T}{\partial y^2} \right] \quad (4)$$

The thermophysical properties of the nanofluid are given as [50]:

$$\rho_{nf} = (1 - \phi)\rho_f + \phi\rho_s \quad (5)$$

$$(\rho C_p)_{nf} = (1 - \phi)(\rho C_p)_f + \phi(\rho C_p)_s \quad (6)$$

$$(\rho\beta)_{nf} = (1 - \phi)(\rho\beta)_f + \phi(\rho\beta)_s \quad (7)$$

$$\frac{k_{nf}}{k_f} = \frac{(k_s + 2k_f) - 2\phi(k_f - k_s)}{(k_s + 2k_f) + \phi(k_f - k_s)} \quad (8)$$

$$\alpha_{nf} = \frac{k_{nf}}{(\rho C_p)_{nf}} \quad (9)$$

$$\mu_{nf} = \frac{\mu_f}{(1 - \phi)^{2.5}} \quad (10)$$

2.3 TRANSFORMATION PARAMETERS

The parameters for transforming the dimensional governing equations to dimensionless equations are as follows [51]:

$$X = \frac{x}{L}, Y = \frac{y}{L}, U = \frac{uL}{\alpha_f}, V = \frac{vL}{\alpha_f}, \varphi = \frac{T - T_c}{T_h - T_c}, P = \frac{\rho L^2}{\rho_{nf} \alpha_f^2}, Pr = \frac{\nu_f}{\alpha_f}. \quad (11)$$

The non-dimensional continuity, momentum, and Energy equations are as follows:

Continuity:

$$\frac{\partial U}{\partial X} + \frac{\partial V}{\partial Y} = 0 \quad (12)$$

X-Momentum:

$$U \frac{\partial U}{\partial X} + V \frac{\partial U}{\partial Y} = -\frac{\partial P}{\partial X} + \frac{\nu_{nf}}{\nu_f} Pr \left[\frac{\partial^2 U}{\partial X^2} + \frac{\partial^2 U}{\partial Y^2} \right] \quad (13)$$

Y-Momentum:

$$U \frac{\partial V}{\partial X} + V \frac{\partial V}{\partial Y} = -\frac{\partial P}{\partial Y} + \frac{\nu_{nf}}{\nu_f} Pr \left[\frac{\partial^2 V}{\partial X^2} + \frac{\partial^2 V}{\partial Y^2} \right] + Ra Pr \frac{(\rho\beta)_{nf}}{\rho_{nf} \beta_f} \varphi \quad (14)$$

Energy:

$$U \frac{\partial \varphi}{\partial X} + V \frac{\partial \varphi}{\partial Y} = \frac{\alpha_{nf}}{\alpha_f} \left[\frac{\partial^2 \varphi}{\partial X^2} + \frac{\partial^2 \varphi}{\partial Y^2} \right] \quad (15)$$

2.3 APPLICABLE BOUNDARY CONDITIONS

The velocity of all the walls are assumed to be $U = V = 0$; The four walls of the cold enclosure are kept at a constant temperature of φ_c , while the walls of the heated rectangular cylinder at a fixed temperature of φ_h .

3. SOLUTION TECHNIQUES

The numerical method employed in the current analysis leverages the finite element formulation of the Galerkin weighted residual method. The space between the enclosure and

the rectangular cylinder was produced applying the Boolean operation, and water-Fe₃O₄ nanofluid was added to the model. The solid boundaries were then subjected to the applicable boundary conditions. The computational domain was then discretized by applying the extremely fine grid size option, and the free triangular mesh model was used to generate the required mesh. The continuity, momentum, and energy transport equations were transformed into a set of integral equations using the Galerkin residual and Gauss quadrature formulations. The needed boundary conditions were then applied to the integrated equations and the Newton-Raphson iterative procedure was used to convert the resulting equations into linear equations. The linear equations were thereafter implemented (in COMSOL Multiphysics 5.5 software) using the triangular factorization method (TFM).

4. EVALUATION OF NUSSELT NUMBER

Nusselt number is a non-dimensional parameter that is used to quantify the rate of heat transfer. The local Nusselt number based on l is given by Eq. (16):

$$Nu_l = -\frac{\partial \phi}{\partial X} \Big|_{X=l} \tag{16}$$

Equally, using some of the dimensionless quantities defined in Eq. (11), the mean Nusselt number on any of the walls of the geometry investigated is given by Eq. (17):

$$\overline{Nu} = \frac{k_{nf}}{k_f} \left[\int_0^1 -\frac{\partial \phi}{\partial X} dY \right] \tag{17}$$

5. RESULTS AND DISCUSSION

5.1 RESULT VALIDATION

In order to validate the COMSOL Multiphysics 5.5 code used in the present study, the results of a differentially heated square enclosure with insulated horizontal walls, in the absence of the rectangular cylinder, in Table 2 are compared to previous works, and the comparison well aligns with those in literature.

Table 2 Mean Nusselt number of the heated wall; comparisons between the present study and the results of other researchers, when $Pr = 0.71$

Rayleigh number	[50]	[52]	[53]	[54]	[55]	Present Study
10^3	1.118	1.105	1.118	1.108	1.114	1.118
10^4	2.245	2.303	2.243	2.201	2.245	2.245
10^5	4.522	4.646	4.519	4.490	4.510	4.522
10^6	8.826	9.012	8.800	8.754	8.806	8.832

5.2 EFFECTS OF VOLUME FRACTION (ϕ) ON ISOTHERMS AND VELOCITY STREAMLINES

Figures 2(a-b) show the effects of volume fraction increment on isothermal and velocity streamline contours for the aspect ratio of 0.5 at $Ra = 10^5$. The changes in the contours were observed from $\phi = 0$ to 0.06 which indicated little alterations in the isothermal contours as

volume fraction increases. The velocity streamlines, however, exhibit changes in contours as the volume fraction increases. For all the contours to the left of the heated rectangular cylinder in the square cavity, no observable changes occurred in the velocity streamlines between $\phi = 0$ and 0.02. But, from $\phi = 0.04$ to 0.06, there is a formation of vortex in the innermost bottom portion of the contours, which increases in size as the volume fraction increases. However, for the contours located to the right of the heated rectangular cylinder, the innermost streamline contour towards the bottom portion was observed to be on the decrease and then separated at $\phi = 0.04$ to form a vortex; further increase in $\phi = 0$ to 0.06 resulted in shrinking of the vortex.

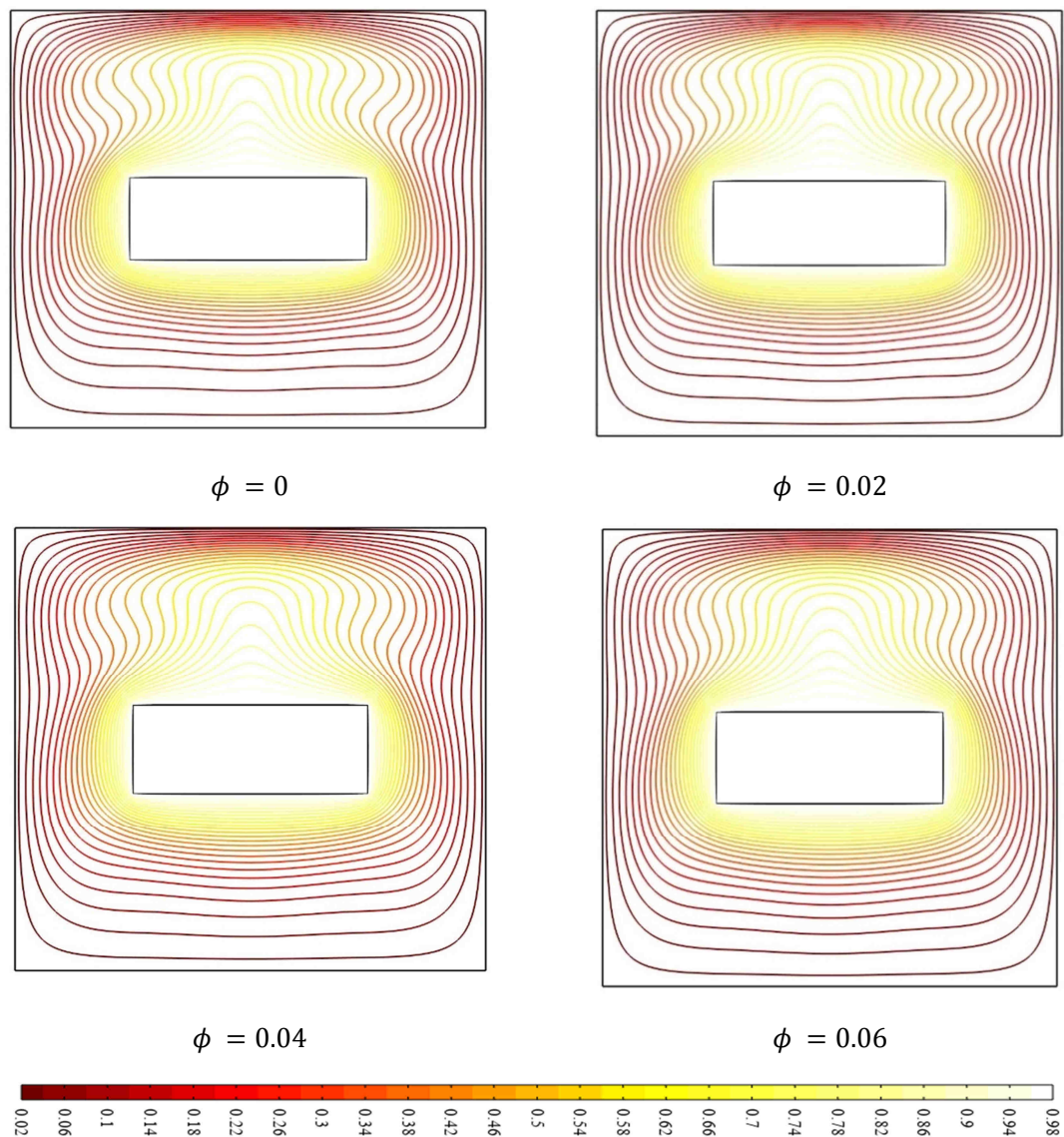


Fig. 2 (a) Isothermal contours at $Ra = 10^5$, and $AR = 0.5$

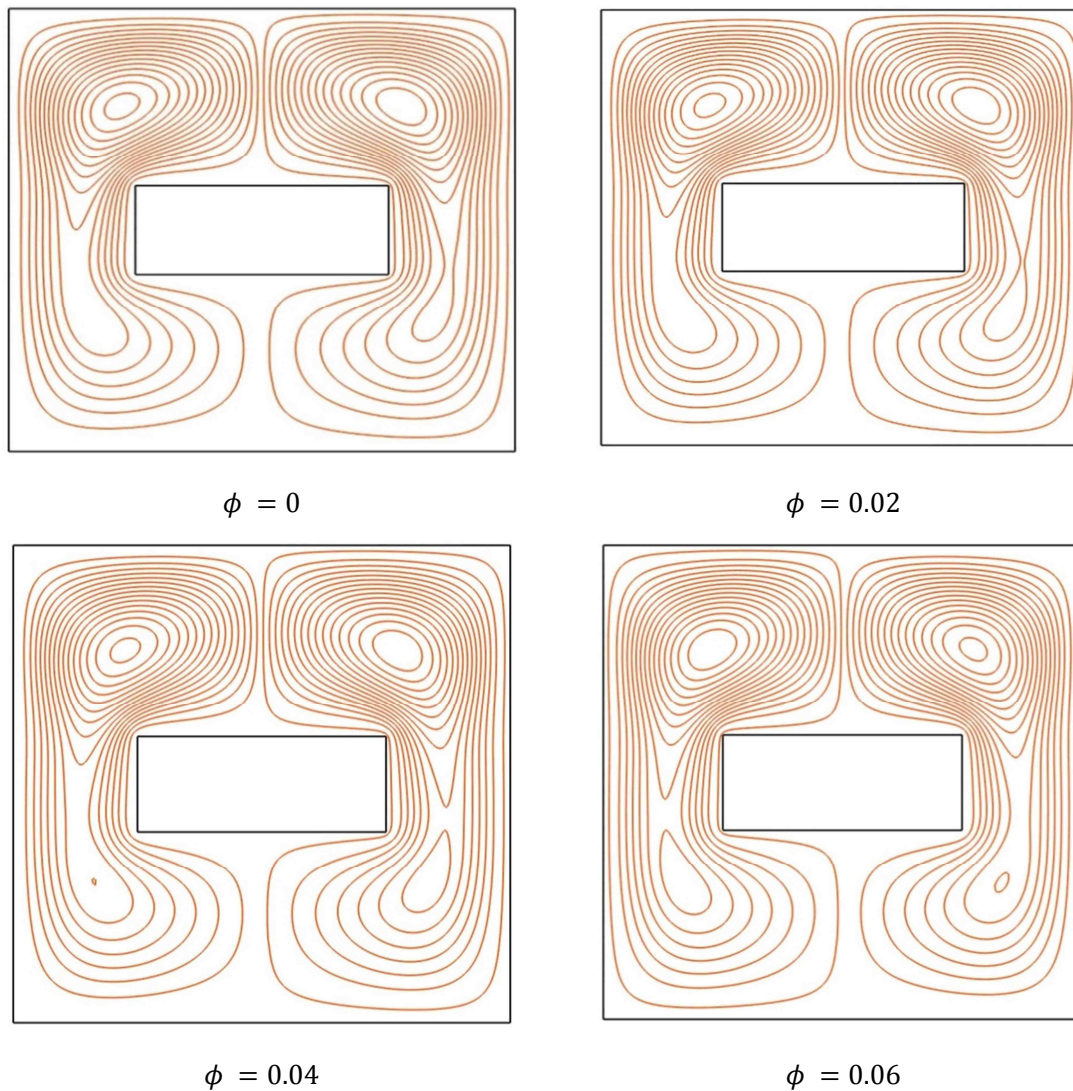


Fig. 2 (b) Velocity Streamlines at $Ra = 10^5$, and $AR = 0.5$

Figures 3(a-b) depict the isothermal and velocity streamlines contours at $Ra = 10^6$ and $AR = 0.5$, for different volume fractions. For the isothermal contours, as the volume fraction of the nanoparticles increased, marginal changes in the shape of the contours around the rectangular cylinder were observed at the bottom portion of the cavity. But significant changes were observed in the density of the contours at the top portion of the cavity which could be due to an increase in the intensity of convection as a result of the increase in thermal conductivity of the nanofluid. For the velocity streamlines, however, an increase in the volume fraction of the nanoparticles from 0 to 0.02 triggered an additional contour at the top right end of the rectangular cylinder. Further increase in volume fraction of the nanoparticles resulted in the formation of denser streamline contours around the upper portion of the cavity. At a maximum value of ϕ , another contour was formed close to the right top end of the rectangular cylinder.

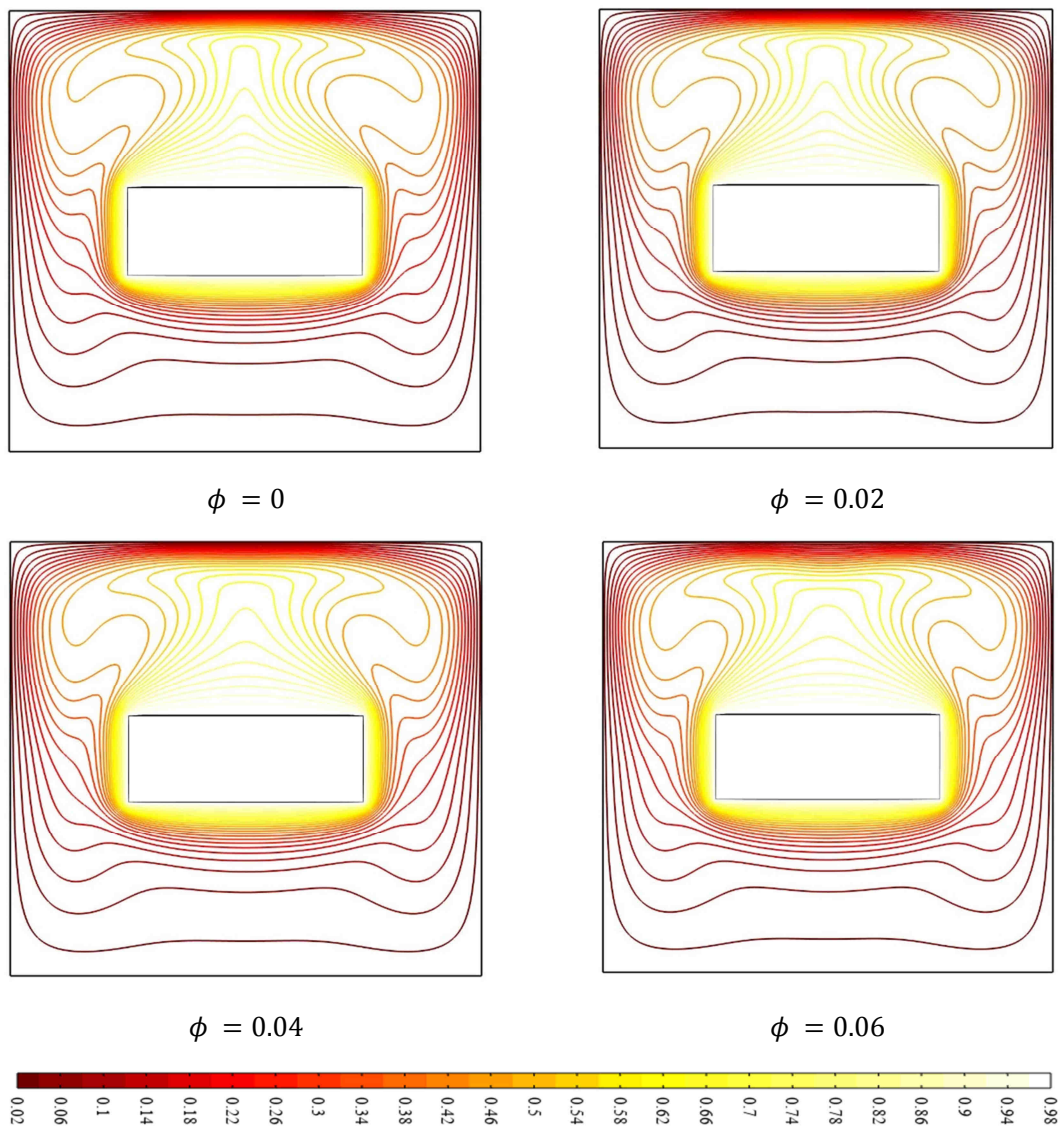
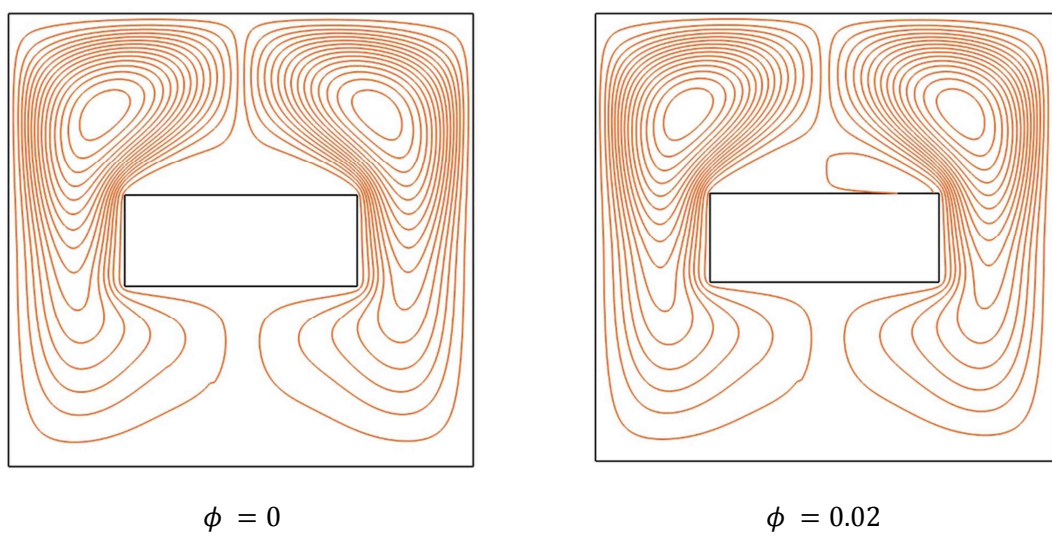


Fig. 3 (a) Isothermal contours at $Ra = 10^6$, and $AR = 0.5$



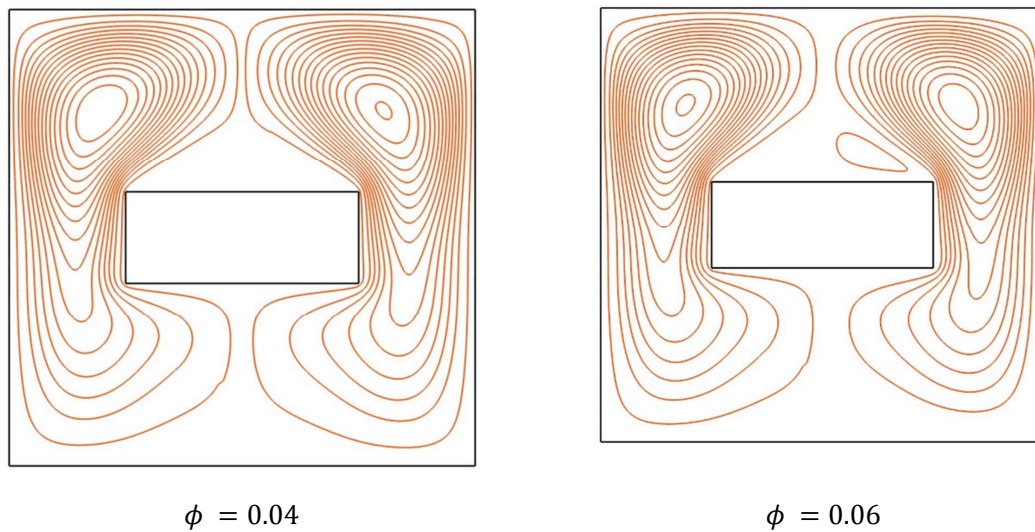


Fig. 3 (b) Velocity Streamlines at $Ra = 10^6$, and $AR = 0.5$.

5.3 EFFECT OF RAYLEIGH NUMBER ON ISOTHERMS AND VELOCITY STREAMLINES

Figures 2 and 3 display the isothermal and velocity streamline contours at $Ra = 10^5$ and 10^6 for $AR = 0.5$. Taking $\phi = 0$ for both Rayleigh numbers, at $Ra = 10^5$, moving from the bottom of the cavity upwards, the isothermal contours and velocity streamline become denser. Furthermore, as the Rayleigh number increases, the isothermal contours move further upwards toward the upper portion of the cavity and the velocity streamlines increase further and the rate of heat transfer becomes enhanced due to the increase in buoyancy effect in the cavity.

5.4 EFFECTS OF ASPECT RATIO AND NANOPARTICLE VOLUME FRACTION ON LOCAL NUSSELT NUMBER

Figures 4(a) show the local Nusselt number profiles for the outer top wall for various volume fractions ($0 \leq \phi \leq 0.06$) and aspect ratios ($0.1 \leq AR \leq 0.7$) at $Ra = 10^6$. For the range of nanoparticle volume fraction considered and for aspect ratio in the range of $0.1 \leq AR \leq 0.5$, along the wall between 0-0.13 and 0.87-1.0, local Nusselt number was found to be independent of nanoparticle addition. Furthermore, for $AR = 0.3$ and ($0 \leq \phi \leq 0.06$), the rate of heat transfer increases with an increase in nanoparticle volume fraction until between 0.4 and 0.6 of the wall length where the addition of nanoparticle results in a decrease in the rate of heat transfer. However, nanoparticle addition resulted in heat transfer augmentation between 0.6 and 0.87 of the wall lengths. The trend of heat transfer when $AR = 0.5$ is similar to that of $AR = 0.3$. At $AR = 0.7$, the rate of heat transfer was observed to be almost independent of nanoparticle volume fraction increment.

The effects of aspect ratio and nanoparticle volume fraction on the local Nusselt number for the outer lower wall are displayed in Figure 4(b). The plots reveal that the local Nusselt number increases with nanofluid volume fraction. For all the ranges of volume fractions and aspect ratios considered, the local Nusselt number for each of the plots attained a local maximum along the wall between 0 and 0.2; and then decreases until it approaches about 40% of the wall length where it assumed a constant local Nusselt number value up to a point which is a function of the aspect ratio of the geometry. Thereafter, it increases and then attains the

same maximum value of the local Nusselt number as the previous and decreases further along the wall.

To examine the behaviour of nanoparticle volume fraction on the vertical walls of the cavity, the local Nusselt number graphs were plotted for various aspect ratios at $Ra = 10^6$, as shown in Figure 5. The plots in Figure 5(a) depict the local Nusselt number profile for the outer right wall where at approximately 0.2 of the wall lengths for $0.1 \leq AR \leq 0.7$, the local Nusselt number attained a maximum value and then reduces further along the length of the wall (except for $AR = 0.7$, which peaked at 0.4 wall length and then attained a local maximum value) and thereafter decreases throughout the remaining length of the wall. The plots in Figure 5(b), which are for the outer left wall, are a mirror image of those in Figure 5(a).

The plots in Figure 6(a) present the local Nusselt number graph for the top wall of the rectangular cylinder. At $AR = 0.1$ and 0.7 , $\phi = 0.06$ exhibits the highest local Nusselt number value as volume fraction increases. For $AR = 0.3$ and 0.5 (very close to the wall ends), nanoparticle addition does not have any significant effect on the rate of heat transfer. Further away from the wall ends, however, volume fraction addition brought about a significant reduction in heat transfer except between 0.1 to 0.2 and 0.2 to 0.3 for $AR = 0.3$ and $AR = 0.5$ respectively where nanoparticle addition results in heat transfer augmentation. The bottom wall local Nusselt number plots for the heated rectangular cylinder are shown in Figure 6(b). $AR = 0.1$ and $0 \leq \phi \leq 0.06$ established the highest local Nusselt number compared to other aspect ratios.

Figure 7 reveals the local Nusselt number graphs when $Ra = 10^6$ for different aspect ratios. The plots show that the local Nusselt number reduces between 0 and 0.15 of the wall lengths and then increases from 0.15 to 0.2 of the wall lengths. In addition, an increase in the local Nusselt number favors a decrease in the aspect ratio. The graphs in Figure 7(b) present the local Nusselt number profile along the inner left wall whose graph's patterns exhibit a mirror image of the inner right wall. Also, Figures 7(a-b) show that the highest heat transfer augmentation occurred at $\phi = 0.06$ for all aspect ratios considered.

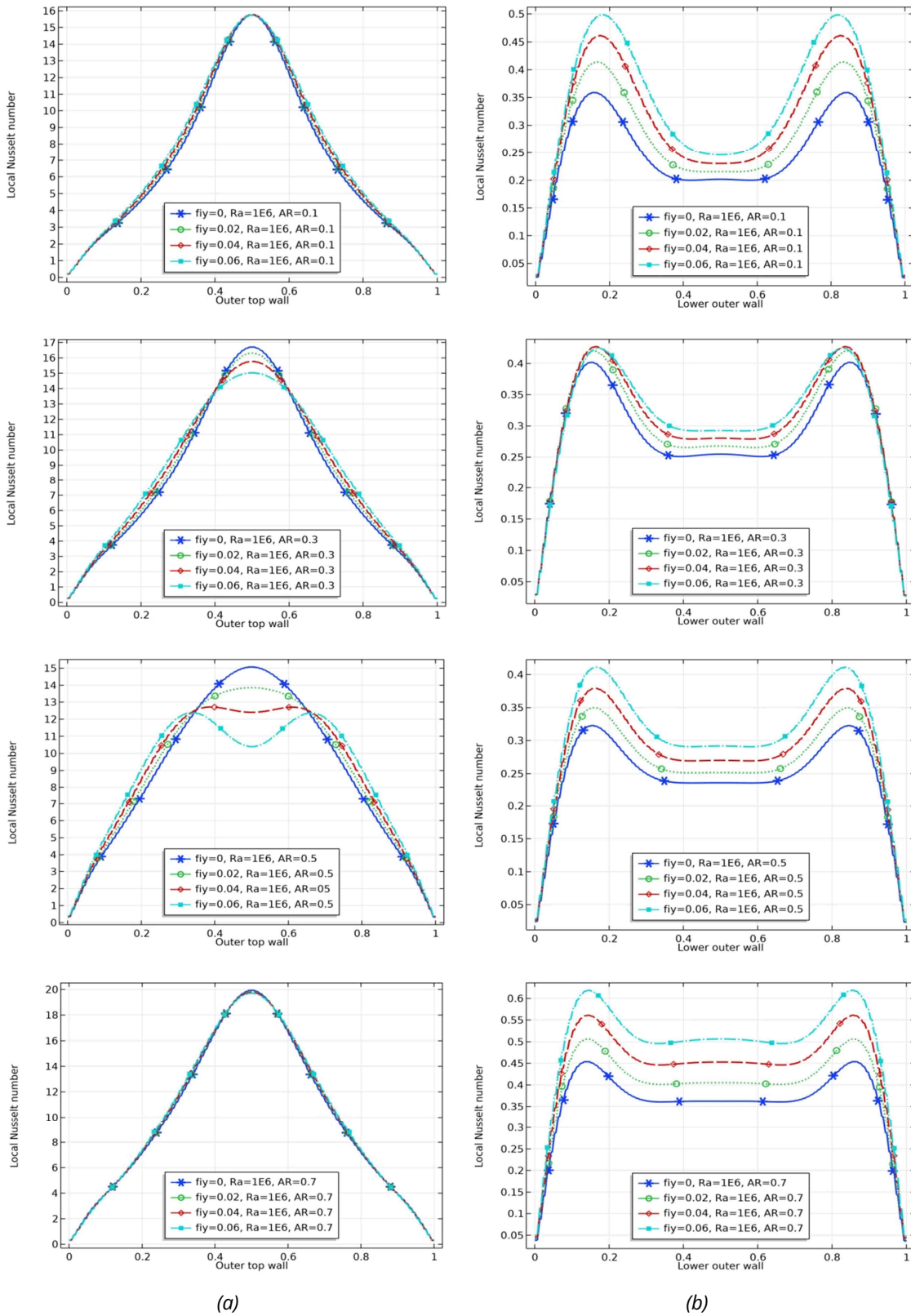


Fig. 4 Local Nusselt number profile for different volume fractions and aspect ratios at $Ra = 10^6$ (a) Outer Top wall, (b) Outer Lower Wall

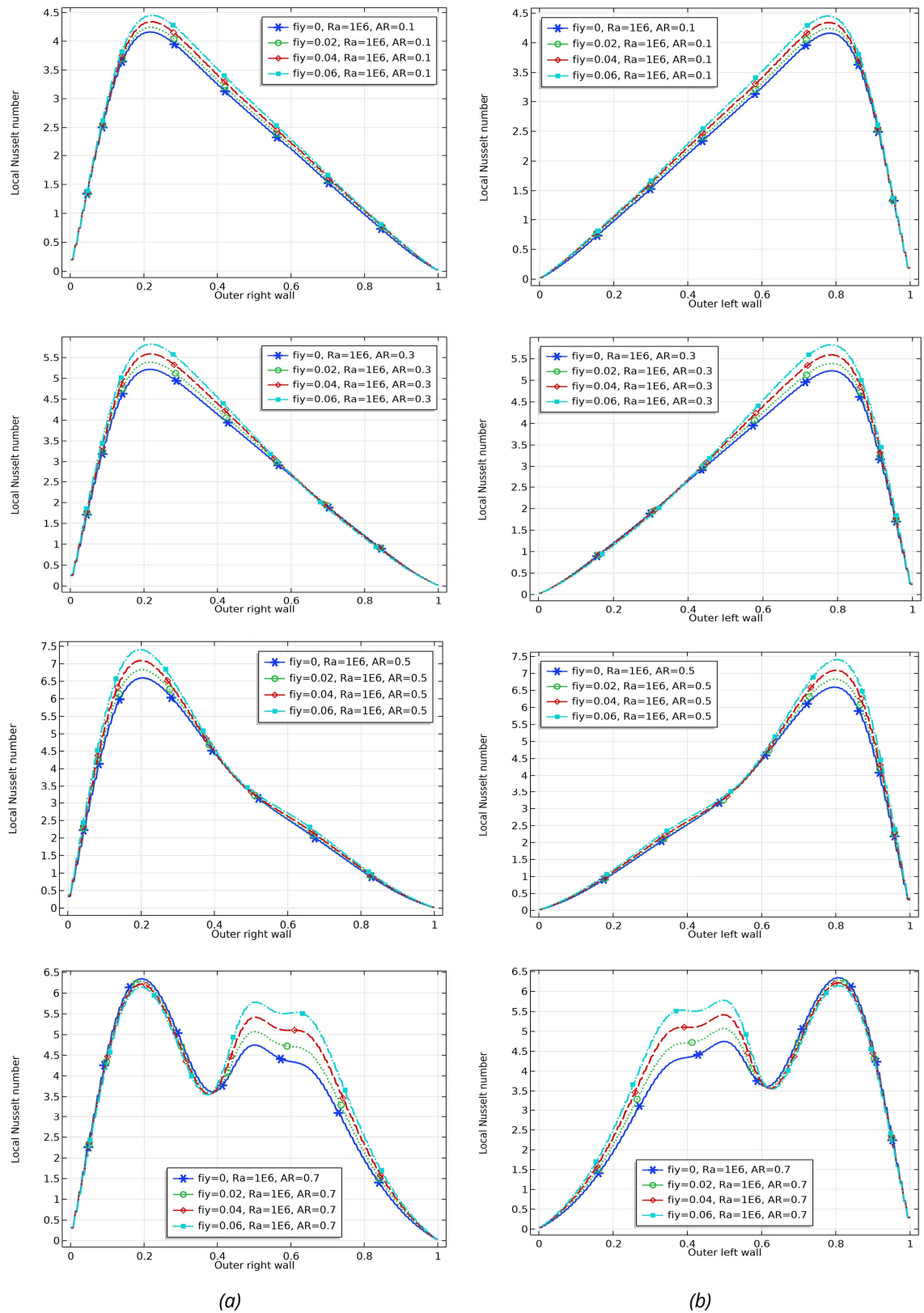


Fig. 5 Local Nusselt number profile for different volume fraction and aspect ratios at $Ra = 10^6$ (a) Outer Right Wall, (b) Outer left wall

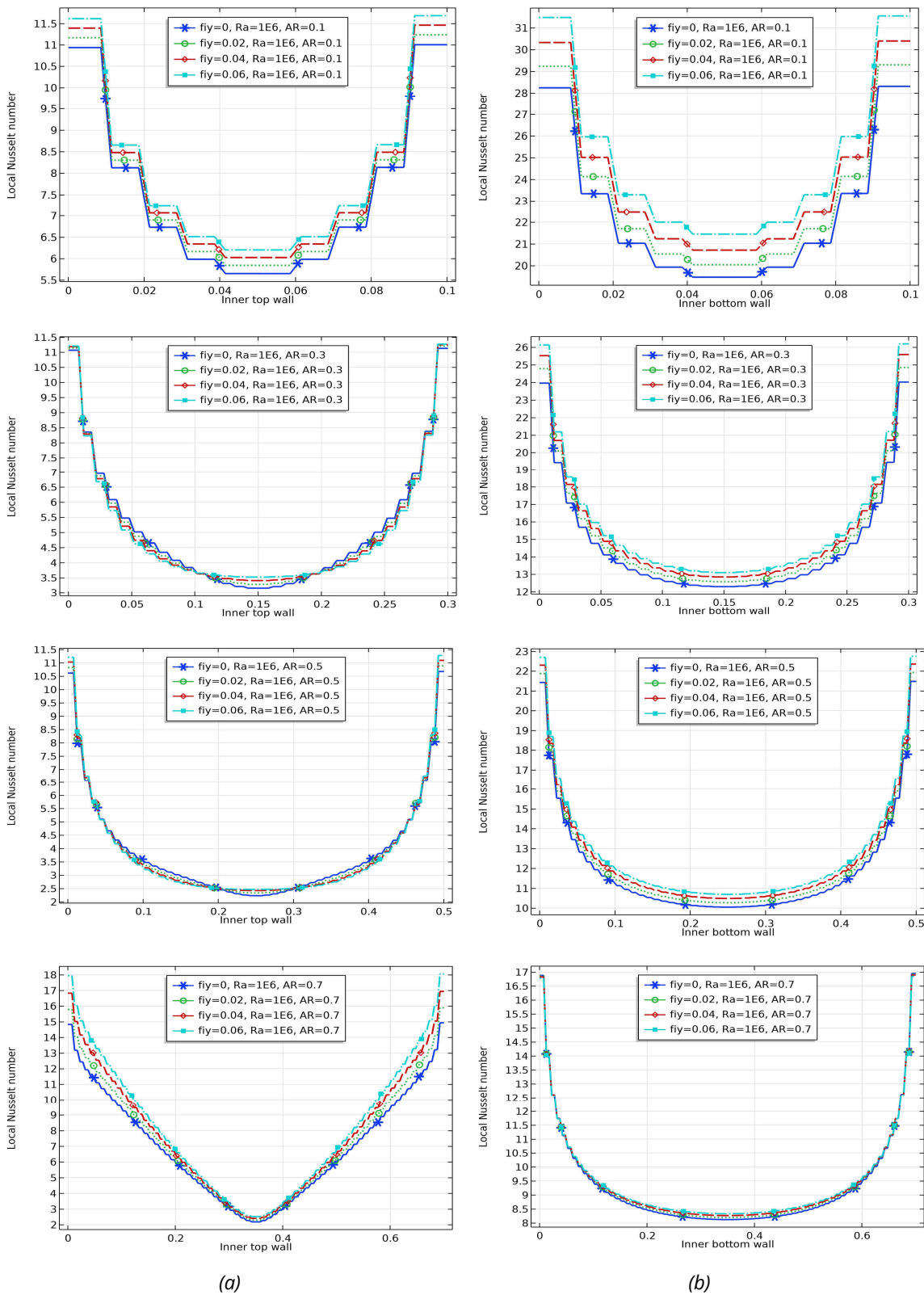


Fig. 6 Local Nusselt number profile for different volume fractions and aspect ratios at $Ra = 10^6$ (a) Inner Top Wall, (b) Inner Bottom Wall

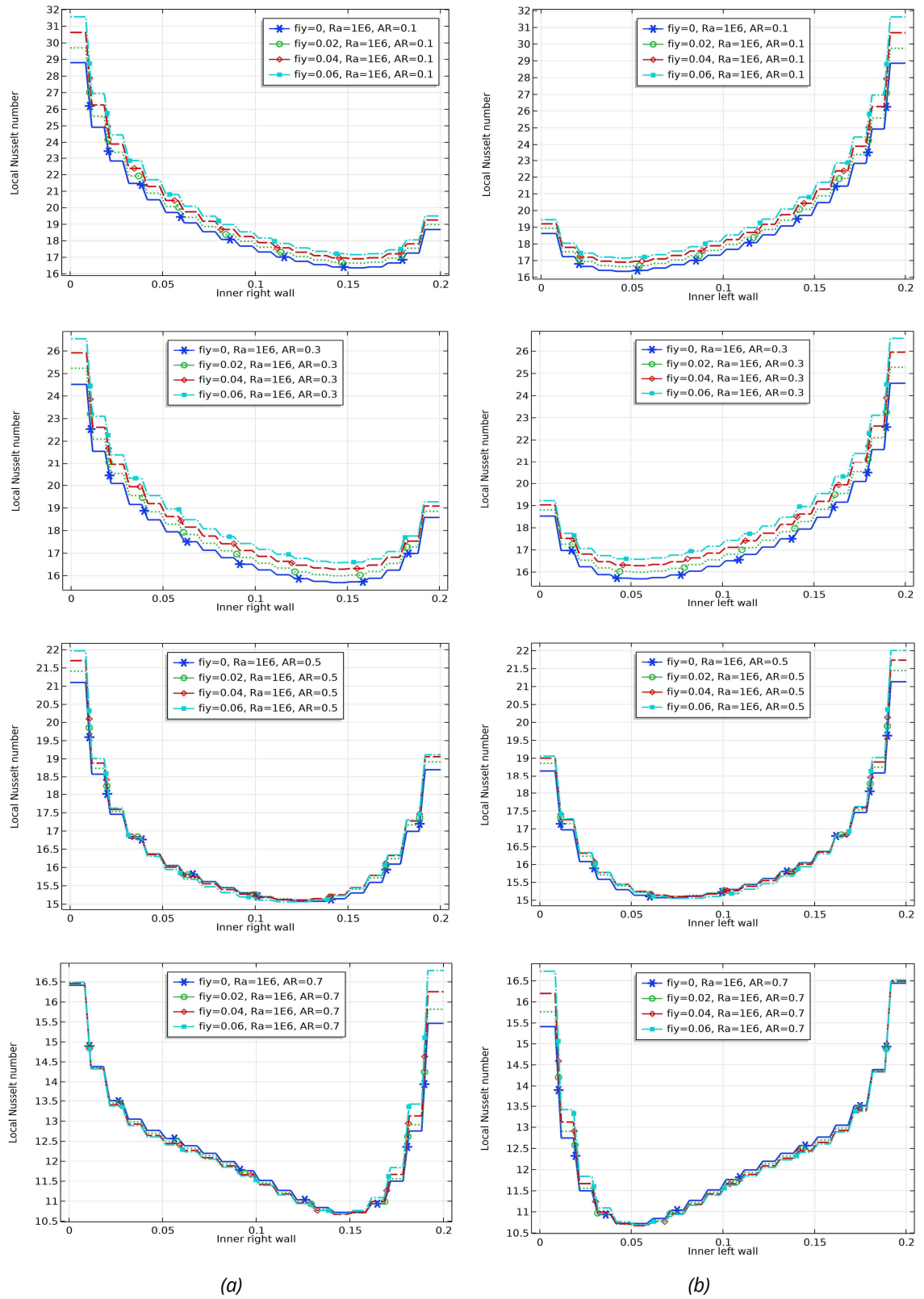


Fig. 7 Local Nusselt number profile for different volume fractions and aspect ratios at $Ra = 10^6$ (a) Inner Right Wall, (b) Inner Left Wall

5.5 EFFECT OF RAYLEIGH NUMBER ON AVERAGE NUSELT NUMBER

The plots for the average Nusselt number of the heated rectangular cylinder against volume fraction for various Rayleigh number values at $AR = 0.5$ are presented in Figure 8. The plots show that there is heat transfer enhancement as Rayleigh number and nanoparticle volume fraction increase and this becomes most significant at $Ra = 10^6$. But for the Rayleigh number lower than 10^5 , the average Nusselt number of the cylinder walls is independent of the Rayleigh number increment. This observation could be due to the fact that the heat transfer mode is conduction dominant.

Figure 9 shows the plots of the average Nusselt number of the cylinder walls versus aspect ratio for nanoparticle volume fraction in the range $0 \leq \phi \leq 0.06$ and $Ra = 10^6$. The average Nusselt number of the cylinder walls increases with aspect ratio and nanofluid volume fraction.

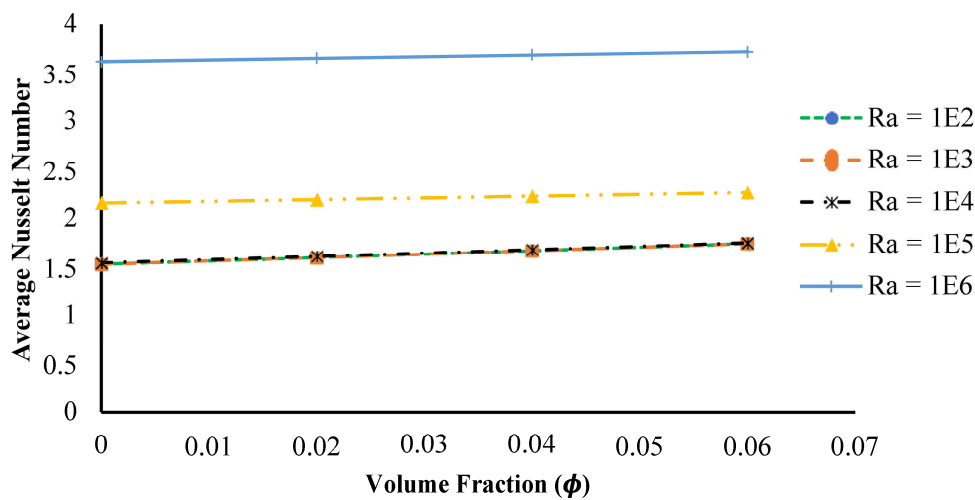


Fig. 8 Average Nusselt number of cylinder walls versus volume fraction for various Rayleigh numbers

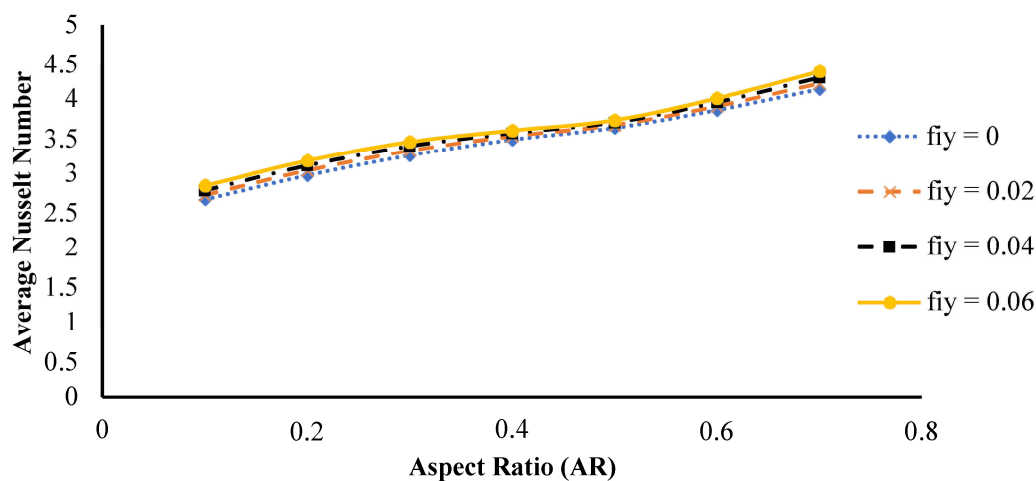


Fig. 9 Average Nusselt number versus aspect ratio for the rectangular cylinder walls for various nanofluid volume fractions

6. CONCLUSIONS

A detailed numerical analysis of the implication of aspect ratio ($0.1 \leq AR \leq 0.7$), nanoparticle volume fraction ($0 \leq \phi \leq 0.06$), and Rayleigh number ($10^2 \leq Ra \leq 10^6$) on velocity streamlines, isothermal contours, local and average Nusselt numbers were analyzed on fluid flow and heat transfer characteristics in a square enclosure with a concentric rectangular cylinder embedded in it. The following major conclusions were made:

1. For nanoparticle volume fraction in the range $0 \leq \phi \leq 0.06$, the average Nusselt number of the walls of the rectangular cylinder were found to be independent of Rayleigh number in the range of $10^2 \leq Ra \leq 10^4$.
2. For flow regimes within Ra in the interval of $10^2 \leq Ra \leq 10^4$, it is advisable to use $Ra = 10^2$ since it gives the same rate of heat transfer; this will ensure a reduction in the cost incurred in heating up the hot walls of the cylinder.
3. Aspect ratio increment ($0.1 \leq AR \leq 0.7$) was found to augment the heat transfer rate of the walls of the rectangular cylinder. Additionally, at $AR = 0.5$, the average Nusselt number of the cylindrical wall is almost insensitive to nanofluid addition, therefore, to reduce the cost incurred from the purchase of nanoparticles, it is advisable to use a very low nanoparticle volume fraction.
4. Nanoparticle volume fraction increment in the range of $0 \leq \phi \leq 0.06$ has a positive effect on heat transfer enhancement.
5. At $Ra = 10^6$ and for the range of aspect ratios considered, the highest local Nusselt number was obtained at the bottom wall of the rectangular cylinder when $\phi = 0.06$.

7. ACKNOWLEDGMENTS

We are grateful to Tertiary Education Trust Fund for providing the fund used in acquiring the Laptop used for this research work.

LIST OF NOTATIONS

- AR - Aspect ratio
 c - Cold
 Cp - Specific heat [$KJkg^{-1}K^{-1}$]
 F - Fluid
 G - Gravitational acceleration [ms^{-1}]
 Gr - Grashof number
 h - Hot
 H - Block height [m]
 K - Thermal conductivity [$Wm^{-1}K^{-1}$]
 l - Local
 L - Dimensionless Height of square cavity
 nf - Nanofluid

- Nu - Local Nusselt number
 \overline{Nu} - Average Nusselt number
 p - Dimensional pressure [Nm^{-2}]
 P - Dimensionless pressure
 Pr - Prandtl number
 Ra - Rayleigh number
 s - Solid
 T - Dimensional temperature [K]
 T_c - Dimensional cold wall temperature [K]
 T_h - Dimensional hot wall temperature [K]
 u, v - Dimensional velocity components [ms^{-1}]
 U, V - Dimensionless velocity components
 W - Block width [m]
 x, y - Dimensional Cartesian coordinates
 X, Y - Dimensionless Cartesian coordinates

Greek Symbols

- α - Thermal diffusivity [m^2s^{-1}]
 β - Thermal expansion [K^{-1}]
 μ - Dynamic viscosity [$kgsm^{-1}$]
 ν - Kinematic Viscosity [Nsm^2]
 ρ - Density [kgm^{-3}]
 ϕ - Volume fraction
 φ - Dimensionless temperature

8. REFERENCES

- [1] A.D. Abdulsahib and K. Al-Farhany, Review of the Effects of Stationary/Rotating Cylinder in a Cavity on the Convection Heat Transfer in Porous Media with/without Nanofluid, *Mathematical Modelling of Engineering Problems*, Vol. 8, No. 3, pp. 356-364, 2021.
<https://doi.org/10.18280/mmep.080304>
- [2] K.K. Al-Chlahawi, H.H. Alaydamee, A.E. Faisal, K. Al-Farhany and M.A. Alomari, Newtonian and non-Newtonian nanofluids with entropy generation in conjugate natural convection of hybrid nanofluid-porous enclosures: A review, *Heat Transfer*, 2021.
<https://doi.org/10.1002/htj.22372>
- [3] F. Redouane, W. Jamshed, S.S.U. Devi, B.M. Amine, R. Safdar, K. Al-Farhany, M.R. Eid, K.S. Nisar, A.-H. Abdel-Aty and I.S. Yahia, Influence of entropy on Brinkman–Forchheimer model of MHD hybrid nanofluid flowing in enclosure containing rotating cylinder and

- undulating porous stratum, *Scientific Reports*, Vol. 11, No. 1, pp. 24316, 2021/12/21, 2021. <https://doi.org/10.1038/s41598-021-03477-4>
- [4] G.H. Kefayati, Lattice boltzmann simulation of natural convection in a square cavity with a linearly heated wall using nanofluid, *Arabian Journal for Science and Engineering*, Vol. 39, No. 3, pp. 2143-2156, 2012. <https://doi.org/10.1007/s13369-013-0748-1>
- [5] P.C. Nidhin, Numerical analysis of natural convection of nano fluids on square enclosures, *International Research Journal of Engineering and Technology (IRJET)*, Vol. 6, No. 9, pp. 942-947, 2019.
- [6] S. Acharya and S.K. Dash, Natural convection in a cavity with undulated walls filled with water-based non-Newtonian power-law CuO-water nanofluid under the influence of the external magnetic field, *Numerical Heat Transfer; Part A: Applications*, Vol. 76, No. 7, pp. 552-575, 2019. <https://doi.org/10.1080/10407782.2019.1644898>
- [7] S. Sivasankaran and K.L. Pan, Natural convection of nanofluids in a cavity with nonuniform temperature distributions on side walls, *Numerical Heat Transfer; Part A: Applications*, Vol. 65, No. 3, pp. 247-268, 2014. <https://doi.org/10.1080/10407782.2013.825510>
- [8] G.A. Sheikhzadeh, A. Arefmanesh, M. H. Kheirkhah and R. Abdollahi, Natural convection of Cu-water nanofluid in a cavity with partially active side walls, *European Journal of Mechanics - B/Fluids*, Vol. 30, No. 2, pp. 166-176, 2011/03/01/, 2011. <https://doi.org/10.1016/j.euromechflu.2010.10.003>
- [9] H.F. Oztop and E. Abu-Nada, Numerical study of natural convection in partially heated rectangular enclosures filled with nanofluids, *International Journal of Heat and Fluid Flow*, Vol. 29, No. 5, pp. 1326-1336, 2008. <https://doi.org/10.1016/j.ijheatfluidflow.2008.04.009>
- [10] C. Revnic, E. Abu-Nada, T. Grosan and I. Pop, Natural convection in a rectangular cavity filled with nanofluids: Effect of variable viscosity, *International Journal of Numerical Methods for Heat and Fluid Flow*, Vol. 28, No. 6, pp. 1410-1432, 2018. <https://doi.org/10.1108/HFF-06-2017-0244>
- [11] Z. Alloui, P. Vasseur and M. Reggio, Natural convection of nanofluids in a shallow cavity heated from below, *International Journal of Thermal Sciences*, Vol. 50, No. 3, pp. 385-393, 2011. <https://doi.org/10.1016/j.ijthermalsci.2010.04.006>
- [12] E. Abu-Nada, Effects of variable viscosity and thermal conductivity of Al₂O₃-water nanofluid on heat transfer enhancement in natural convection, *International Journal of Heat and Fluid Flow*, Vol. 30, No. 4, pp. 679-690, 2009. <https://doi.org/10.1016/j.ijheatfluidflow.2009.02.003>
- [13] A.I. Alsabery, T. Tayebi, A.J. Chamkha and I. Hashim, Effects of non-homogeneous nanofluid model on natural convection in a square cavity in the presence of conducting solid block and corner heater, *Energies*, Vol. 11, No. 10, 2018. <https://doi.org/10.3390/en11102507>
- [14] G.A. Sheikhzadeh, M. Nikfar and A. Fattahi, Numerical study of natural convection and entropy generation of Cu-water nanofluid around an obstacle in a cavity, *Journal of Mechanical Science and Technology*, Vol. 26, No. 10, pp. 3347-3356, 2012.

<https://doi.org/10.1007/s12206-012-0805-9>

- [15] A.D. Abdulsahib and K. Al-Farhany, Numerical Investigation of the nanofluid mixed convection on two layers enclosure with rotating cylinder: High Darcy Number Effects, IOP Conference Series: *Materials Science and Engineering*, Vol. 928, 2nd International Scientific Conference of Al-Ayen University (ISCAU-2020) 15-16 July 2020, Thi-Qar, Iraq, 2020. <https://doi.org/10.1088/1757-899X/928/2/022001>
- [16] G.Y. Kahwaji and O. Ali, Numerical Investigation of Natural Convection Heat Transfer from Square Cylinder in an Enclosed Enclosure Filled with Nanofluids, *International Journal of Recent advances in Mechanical Engineering (IJMECH)*, Vol.4, No.4, 2015. <https://doi.org/10.14810/ijmech.2015.4401>
- [17] A.H. Pordanjani, A. Jahanbakhshi, A. Ahmadi Nadooshan and M. Afrand, Effect of two isothermal obstacles on the natural convection of nanofluid in the presence of magnetic field inside an enclosure with sinusoidal wall temperature distribution, *International Journal of Heat and Mass Transfer*, Vol. 121, pp. 565-578, 2018. <https://doi.org/10.1016/j.ijheatmasstransfer.2018.01.019>
- [18] A.H. Mahmoudi, M. Shahi, A.H. Raouf and A. Ghasemian, Numerical study of natural convection cooling of horizontal heat source mounted in a square cavity filled with nanofluid, *International Communications in Heat and Mass Transfer*, Vol. 37, No. 8, pp. 1135-1141, 2010. <https://doi.org/10.1016/j.icheatmasstransfer.2010.06.005>
- [19] Y. Ma, R. Mohebbi, M.M. Rashidi and Z. Yang, Simulation of nanofluid natural convection in a U-shaped cavity equipped by a heating obstacle: Effect of cavity's aspect ratio, *Journal of the Taiwan Institute of Chemical Engineers*, Vol. 93, pp. 263-276, 2018. <https://doi.org/10.1016/j.jtice.2018.07.026>
- [20] Y. Ma, R. Mohebbi, M.M. Rashidi, Z. Yang and M.A. Sheremet, Numerical study of MHD nanofluid natural convection in a baffled U-shaped enclosure, *International Journal of Heat and Mass Transfer*, Vol. 130, pp. 123-134, 2019. <https://doi.org/10.1016/j.ijheatmasstransfer.2018.10.072>
- [21] N.S. Gibanov, I.V. Miroshnichenko and M.A. Sheremet, Comparison of two numerical approaches for natural convection in cavities with energy sources, *Journal of Physics: Conference Series*, Vol. 1382, XXXV Siberian Thermophysical Seminar 27-29 August 2019, Novosibirsk, Russia. <https://doi.org/10.1088/1742-6596/1382/1/012131>
- [22] H. Khakrah, P. Hooshmand, M.Y. Abdollahzadeh Jamalabadi and S. Azar, Thermal lattice Boltzmann simulation of natural convection in a multi-pipe sinusoidal-wall cavity filled with Al₂O₃-EG nanofluid, *Powder Technology*, Vol. 356, pp. 240-252, 2019. <https://doi.org/10.1016/j.powtec.2019.08.013>
- [23] G. Kefayati, Lattice Boltzmann simulation of double-diffusive natural convection of viscoplastic fluids in a porous cavity, *Physics of Fluids*, Vol. 31, No. 1, 2019. <https://doi.org/10.1063/1.5074089>
- [24] H. Nemati, M. Farhadi, K. Sedighi, H.R. Ashorynejad and E. Fattahi, Magnetic field effects on natural convection flow of nanofluid in a rectangular cavity using the Lattice Boltzmann model, *Scientia Iranica*, Vol. 19, No. 2, pp. 303-310, 2012. <https://doi.org/10.1016/j.scient.2012.02.016>

- [25] H.M. Elshehabey, F.M. Hady, S.E. Ahmed and R.A. Mohamed, Numerical investigation for natural convection of a nanofluid in an inclined L-shaped cavity in the presence of an inclined magnetic field, *International Communications in Heat and Mass Transfer*, Vol. 57, pp. 228-238, 2014. <https://doi.org/10.1016/j.icheatmasstransfer.2014.07.004>
- [26] Z.A.S. Raizah, A.M. Aly and S.E. Ahmed, Natural convection flow of a power-law non-Newtonian nanofluid in inclined open shallow cavities filled with porous media, *International Journal of Mechanical Sciences*, Vol. 140, pp. 376-393, 2018. <https://doi.org/10.1016/j.ijmecsci.2018.03.017>
- [27] A. Bendaraa, M.M. Charafi and A. Hasnaoui, Numerical modeling of natural convection in horizontal and inclined square cavities filled with nanofluid in the presence of magnetic field, *European Physical Journal Plus*, Vol. 134, No. 9, 2019. <https://doi.org/10.1140/epjp/i2019-12814-8>
- [28] W. Liu, A. Shahsavari, A.A. Barzinji, A.A.A.A. Al-Rashed and M. Afrand, Natural convection and entropy generation of a nanofluid in two connected inclined triangular enclosures under magnetic field effects, *International Communications in Heat and Mass Transfer*, Vol. 108, 2019. <https://doi.org/10.1016/j.icheatmasstransfer.2019.104309>
- [29] F. Selimefendigil and H.F. Öztop, Effects of conductive curved partition and magnetic field on natural convection and entropy generation in an inclined cavity filled with nanofluid, *Physica A: Statistical Mechanics and its Applications*, Vol. 540, 2020. <https://doi.org/10.1016/j.physa.2019.123004>
- [30] Z.A.S. Raizah and A.M. Aly, Natural convection from heated shape in nanofluid-filled cavity using incompressible smoothed particle hydrodynamics, *Journal of Thermophysics and Heat Transfer*, Vol. 33, No. 4, pp. 917-931, 2019. <https://doi.org/10.2514/1.T5665>
- [31] Z. Li, A. Shafee, M. Ramzan, H.B. Rokni and Q.M. Al-Mdallal, Simulation of natural convection of Fe₃O₄-water ferrofluid in a circular porous cavity in the presence of a magnetic field, *European Physical Journal Plus*, Vol. 134, No. 2, 2019. <https://doi.org/10.1140/epjp/i2019-12433-5>
- [32] M.H. Toosi and M. Siavashi, Two-phase mixture numerical simulation of natural convection of nanofluid flow in a cavity partially filled with porous media to enhance heat transfer, *Journal of Molecular Liquids*, Vol. 238, pp. 553-569, 2017. <https://doi.org/10.1016/j.molliq.2017.05.015>
- [33] B.M. Al-Srayyih, S. Gao and S.H. Hussain, Natural convection flow of a hybrid nanofluid in a square enclosure partially filled with a porous medium using a thermal non-equilibrium model, *Physics of Fluids*, Vol. 31, No. 4, 2019. <https://doi.org/10.1063/1.5080671>
- [34] S. Hussain and S.E. Ahmed, Steady natural convection in open cavities filled with a porous medium utilizing Buongiorno's nanofluid model, *International Journal of Mechanical Sciences*, Vol. 157-158, pp. 692-702, 2019/07/01/, 2019. <https://doi.org/10.1016/j.ijmecsci.2018.10.071>
- [35] A.I. Alsabery, R. Mohebbi, A.J. Chamkha and I. Hashim, Effect of local thermal non-equilibrium model on natural convection in a nanofluid-filled wavy-walled porous cavity

- containing inner solid cylinder, *Chemical Engineering Science*, Vol. 201, pp. 247-263, 2019. <https://doi.org/10.1016/j.ces.2019.03.006>
- [36] K. Al-Farhany and A.D. Abdulsahib, Study of mixed convection in two layers of saturated porous medium and nanofluid with rotating circular cylinder, *Progress in Nuclear Energy*, Vol. 135, 2021. <https://doi.org/10.1016/j.pnucene.2021.103723>
- [37] K. Al-Farhany, K.K. Al-Chlahawi, M.F. Al-dawody, N. Biswas and A.J. Chamkha, Effects of fins on magnetohydrodynamic conjugate natural convection in a nanofluid-saturated porous inclined enclosure, *International Communications in Heat and Mass Transfer*, Vol. 126, 2021. <https://doi.org/10.1016/j.icheatmasstransfer.2021.105413>
- [38] K. Al-Farhany, M.F. Al-dawody, D.A. Hamzah, W. Al-Kouz and Z. Said, Numerical investigation of natural convection on Al₂O₃-water porous enclosure partially heated with two fins attached to its hot wall: under the MHD effects, *Applied Nanoscience (Switzerland)*, 2021. <https://doi.org/10.1007/s13204-021-01855-y>
- [39] N.S. Bondareva, M.A. Sheremet, H.F. Öztöp and N. Abu-Hamdeh, Transient natural convection in a partially open trapezoidal cavity filled with a water-based nanofluid under the effects of Brownian diffusion and thermophoresis, *International Journal of Numerical Methods for Heat and Fluid Flow*, Vol. 28, No. 3, pp. 606-623, 2018. <https://doi.org/10.1108/HFF-04-2017-0170>
- [40] K.F.U. Ahmed, R. Nasrin and M. Elias, Natural convective flow in circular and arc cavities filled with water-Cu nanofluid: A comparative study, *Journal of Naval Architecture and Marine Engineering*, Vol. 15, No. 1, pp. 37-52, 2018. <https://doi.org/10.3329/jname.v15i1.33549>
- [41] A. Pilkington and B. Rosic, LES of natural convection in a closed cavity, In book: *Direct and Large-Eddy Simulation XI, ERCOFTAC Series*, Springer, pp. 307-313, 2019. https://doi.org/10.1007/978-3-030-04915-7_41
- [42] A.E.M. Bouchoucha, R. Bessaïh, H.F. Öztöp, K. Al-Salem and F. Bayrak, Natural convection and entropy generation in a nanofluid filled cavity with thick bottom wall: Effects of non-isothermal heating, *International Journal of Mechanical Sciences*, Vol. 126, pp. 95-105, 2017. <https://doi.org/10.1016/j.ijmecsci.2017.03.025>
- [43] Z. Boulahia, A. Wakif, A.J. Chamkha and R. Sehaqui, Numerical study of natural and mixed convection in a square cavity filled by a Cu-water nanofluid with circular heating and cooling cylinders, *Mechanics and Industry*, Vol. 18, No. 5, 2017. <https://doi.org/10.1051/meca/2017021>
- [44] Q. Yu, Y. Lu, C. Zhang, Y. Wu and B. Sunden, Experimental and numerical study of natural convection in bottom-heated cylindrical cavity filled with molten salt nanofluids, *Journal of Thermal Analysis and Calorimetry*, Vol. 141, No. 3, pp. 1207-1219, 2020. <https://doi.org/10.1007/s10973-019-09112-9>
- [45] M. Sannad, B. Abourida, L. Belarche, H. Doghmi and Mouzaouit, Natural convection in a three-dimensional cavity filled with nanofluid and partially heated: Effect of the heating section dimension, IOP Conference Series: *Materials Science and Engineering*, Vol. 186, XII Maghreb Days of Material Sciences 19–21 November 2015, Fez, Morocco, 2015. <https://doi.org/10.1088/1757-899X/186/1/012032>

- [46] M. Ghalambaz, A. Doostani, E. Izadpanahi and A.J. Chamkha, Conjugate natural convection flow of Ag–MgO/water hybrid nanofluid in a square cavity, *Journal of Thermal Analysis and Calorimetry*, Vol. 139, No. 3, pp. 2321-2336, 2020.
<https://doi.org/10.1007/s10973-019-08617-7>
- [47] R. Mohebbi, S.A.M. Mehryan, M. Izadi and O. Mahian, Natural convection of hybrid nanofluids inside a partitioned porous cavity for application in solar power plants, *Journal of Thermal Analysis and Calorimetry*, Vol. 137, No. 5, pp. 1719-1733, 2019.
<https://doi.org/10.1007/s10973-019-08019-9>
- [48] A.M. Rashad, A.J. Chamkha, M.A. Ismael and T. Salah, Magneto hydrodynamics Natural Convection in a Triangular Cavity Filled with a Cu-Al₂O₃/Water Hybrid Nanofluid with Localized Heating from below and Internal Heat Generation, *Journal of Heat Transfer*, Vol. 140, No. 7, 2018. <https://doi.org/10.1115/1.4039213>
- [49] O.A. Olayemi, A.F. Khaled, O.J. Temitope, O.O. Victor, C.B. Odetunde and I.K. Adegun, Parametric study of natural convection heat transfer from an inclined rectangular cylinder embedded in a square enclosure, *Australian Journal of Mechanical Engineering*, 2021. <https://doi.org/10.1080/14484846.2021.1913853>
- [50] K. Khanafer, K. Vafai and M. Lightstone, Buoyancy-driven heat transfer enhancement in a two-dimensional enclosure utilizing nanofluids, *International Journal of Heat and Mass Transfer*, Vol. 46, No. 19, pp. 3639-3653, 2003.
[https://doi.org/10.1016/S0017-9310\(03\)00156-X](https://doi.org/10.1016/S0017-9310(03)00156-X)
- [51] C.C. Cho, Heat transfer and entropy generation of mixed convection flow in Cu-water nanofluid-filled lid-driven cavity with wavy surface, *International Journal of Heat and Mass Transfer*, Vol. 119, pp. 163-174, 2018.
<https://doi.org/10.1016/j.ijheatmasstransfer.2017.11.090>
- [52] T. Fusegi, J.M. Hyun and K. Kuwahara, Three-dimensional numerical simulation of periodic natural convection in a differentially heated cubical enclosure, *Applied Scientific Research*, Vol. 49, No. 3, pp. 271-282, 1992. <https://doi.org/10.1007/BF00384627>
- [53] G. De Vahl Davis, Natural convection of air in a square cavity: A bench mark numerical solution, *International Journal for numerical methods in fluids*, Vol. 3, No. 3, pp. 249-264, 1983. <https://doi.org/10.1002/flid.1650030305>
- [54] N.C. Markatos and K.A. Pericleous, Laminar and turbulent natural convection in an enclosed cavity, *International Journal of Heat and Mass Transfer*, Vol. 27, No. 5, pp. 755-772, 1984. [https://doi.org/10.1016/0017-9310\(84\)90145-5](https://doi.org/10.1016/0017-9310(84)90145-5)
- [55] G. Barakos, E. Mitsoulis and D. Assimacopoulos, Natural convection flow in a square cavity revisited: Laminar and turbulent models with wall functions, *International Journal for Numerical Methods in Fluids*, Vol. 18, No. 7, pp. 695-719, 1994.
<https://doi.org/10.1002/flid.1650180705>